

1

# Supplementary information

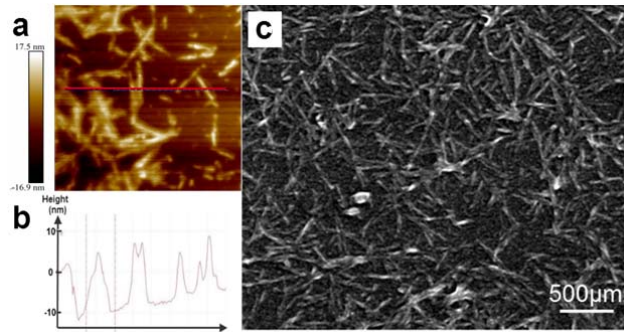
2

3

4

5

## 6 Supplementary Figure 1



7

### 8 Supplementary Figure 1 | Characterization of the lysozyme fibrils by atomic force microscopy

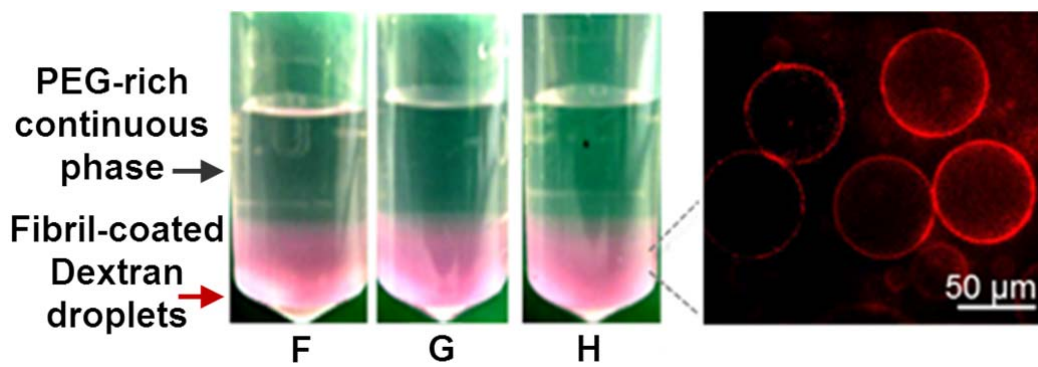
9 (AFM) and scanning electron microscopy (SEM). (a) & (b) The height of lysozyme mature fibrils is

10 15 nm on average, measured by AFM. (c) A SEM image reveals that the average length of

11 lysozyme fibrils is around 600 nm.

12

## 13 Supplementary Figure 2



14

### 15 Supplementary Figure 2 | Supporting evidences showing that almost complete accumulation of

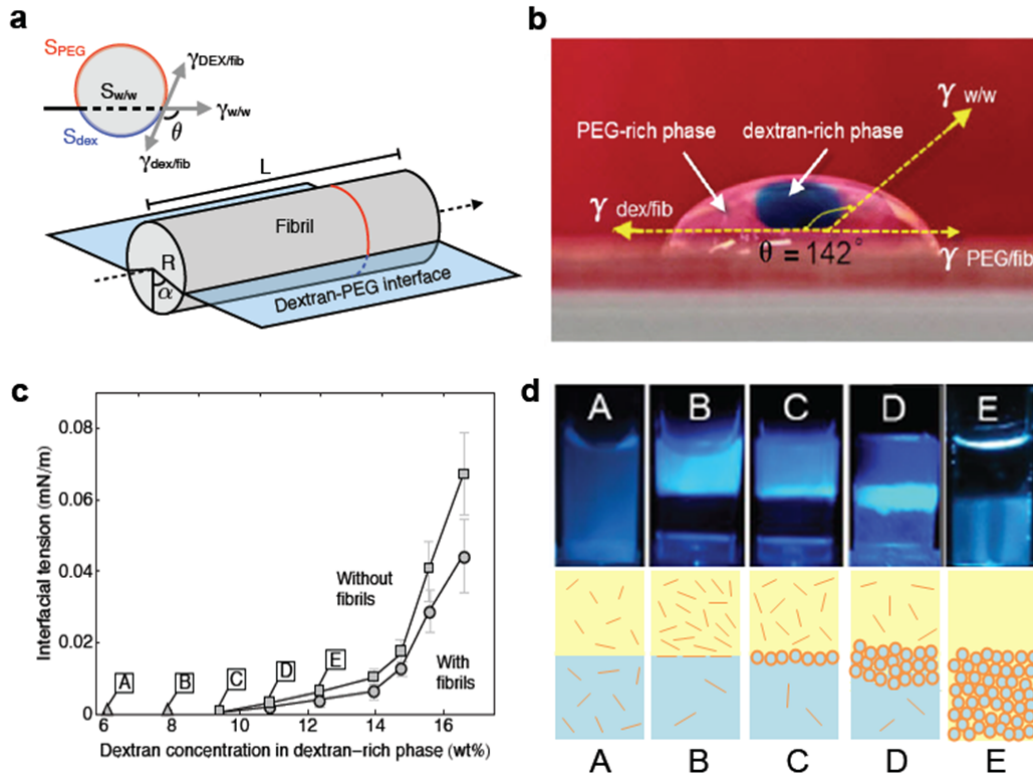
16 **0.05 wt% lysozyme fibrils at the interface of W/W emulsion droplets. (a)** In a solution mixture  
17 containing Nile Red-labelled fibrils and dextran-in-PEG emulsion droplets, a colorless PEG-rich  
18 continuous phase is observed after the sedimentation of dextran-in-PEG emulsion droplets. The  
19 concentrations of dextran in the dextran-rich bottom phases are 13.9%, 14.3% 15.0% for samples  
20 F, G and H, respectively. **b,** A fluorescence microscope image confirms that dyed fibrils  
21 accumulate at the droplet interface.

22

23 When the amount of fibrils is insufficient to cover the created interfacial area of W/W  
24 emulsions, almost all the fibrils go to the interface and only a very little amount of fibrils go to  
25 the bulk phases. Experimentally, fibrils with a low concentration of less than 0.08 wt% is labelled  
26 with Nile red for direct imaging of the distribution of fibrils under natural light. After  
27 homogenization, stable dextran-in-PEG droplets sink down to the bottom of the vial due to  
28 gravity. Consequently, a colorless PEG-rich phase appears on the top (Supplementary Figure 2).  
29 When a blue laser is used to excite Nile Red, a red color is emitted from the W/W interface,  
30 suggesting the accumulation of fibrils at the interface of the emulsion droplets.

31

32 **Supplementary Figure 3**



33

34 **Supplementary Figure 3 | Effect of interfacial tension on the stability of the fibril-coated**

35 **dextran-in-PEG emulsions.** (a), Graphical representation of a single fibril adsorbed at the W/W

36 interface. (b), The wetting angle of a dextran-rich droplet at the interface between a fibril film

37 and a PEG-rich phase is about 142°. (c), Interfacial tension between two aqueous phases,  $\gamma_{w/w}$ ,

38 increases as the equilibrium concentrations of the PEG-rich and dextran-rich phases increase (see

39 square dots in figure S5c). After the adsorption of fibrils, the interfacial tension slightly reduces

40 (round dots in figure S5c. (d), With decreasing interfacial tensions from sample E to A, the

41 sedimentary dextran-in-PEG emulsions become less stable. Correspondingly, more fibrils detach

42 from the droplet interface and migrate to the PEG-rich top phase, as indicated from the

43 fluorescence of ThT-bounded fibrils from sample E to B. For sample E, the dextran-rich emulsions

44 sink down at the bottom of the vial due to gravity, so the fluorescence signals are only observed

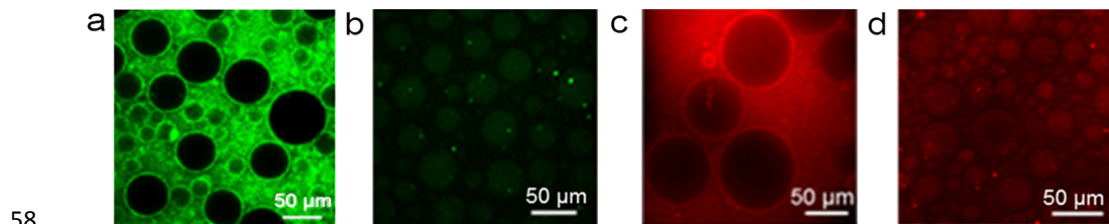
45 at the bottom of the vial. For sample A, fibrils distribute evenly in the mixture since their

46 interaction with the W/W interface is weak compared to the thermal energy of a few  $kT$ .

47 As the interfacial tension  $\gamma_{W/W}$  decreases, the desorption energy of fibrils from the W/W  
48 interface decreases, resulting in the declining stability of dextran-in-PEG emulsions. In our  
49 experiment, we reduced the interface tension by decreasing the concentration of dextran and  
50 PEG in the emulsion mixture while keeping an equal volume of the dextran-rich phase and  
51 PEG-rich phases. The dextran-in-PEG emulsions are found to destabilize faster as the interfacial  
52 tension decreases; correspondingly, more desorbed fibrils leave the droplet interface and enter  
53 the PEG-rich phase, as shown by the fluorescence of ThT-labeled fibrils from sample E to A in  
54 figure S5d. For each sample, a schematic figure is drawn below to illustrate that the decreased  
55 emulsion stability is due to the decreased adsorption of fibrils at the droplet interface.

56

#### 57 **Supplementary Figure 4**



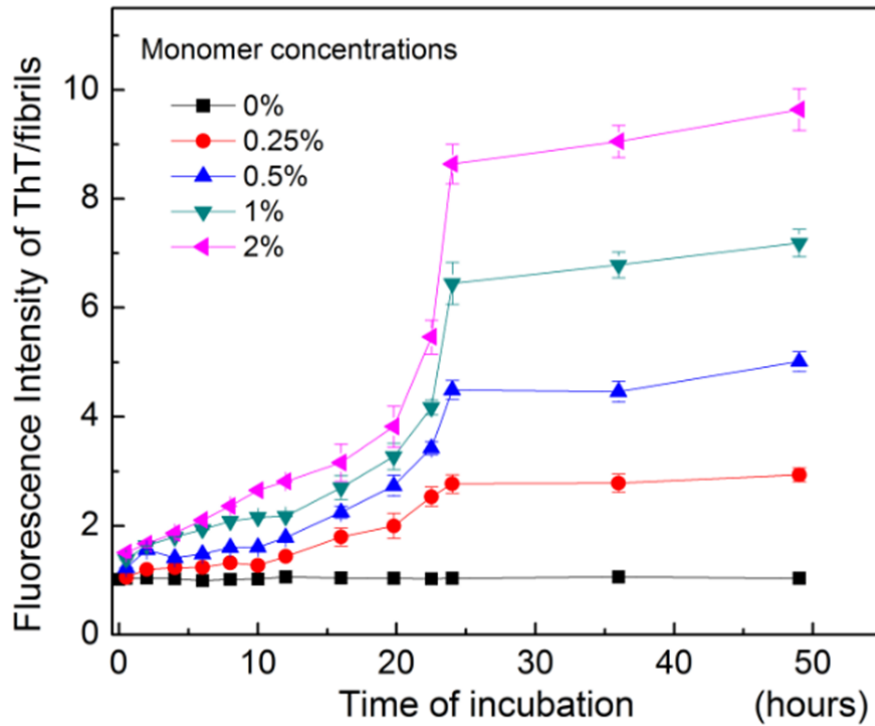
59 **Supplementary Figure 4 | Desorbed lysozyme fibrils preferentially enter the PEG-rich phase**  
60 **rather than the dextran-rich phase.** When the amount of fibrils added is larger than that  
61 required to cover the droplet interface, the remaining non-adsorbed fibrils preferentially enter  
62 the PEG-rich phase. To visualize the lysozyme fibrils in this condition, we labelled the fibrils with  
63 (a) ThT and (c) Nile red. Their partitioning to both the emulsion interfaces and the PEG-rich phase  
64 can be confirmed by the fluorescence microscope images. In comparison, without addition of  
65 fibrils, the dye of (b) ThT and (d) Nile red do not exhibit observable partitioning effects in either

66 the PEG-rich phase or the W/W interface.

67

68 **Supplementary Figure 5**

69



70

71 **Supplementary Figure 5 | Seeded growth of the fibril layers at all-aqueous interfaces is**

72 **quantitatively studied by adding monomeric lysozyme at different concentrations.** The total

73 amount of fibrils at different time points is determined by measuring the intensity of

74 fluorescence of ThT-labeled fibrils.

75

76 In our experiment, we first dissolve 2% dextran, 8% PEG and 0.05% fibrils in 200

77 mM HCl solution by vortex mixing, obtaining dextran-in-PEG emulsion stabilized by

78 fibril monolayers. We then add lysozyme monomers (0 wt%- 2 wt%) into the

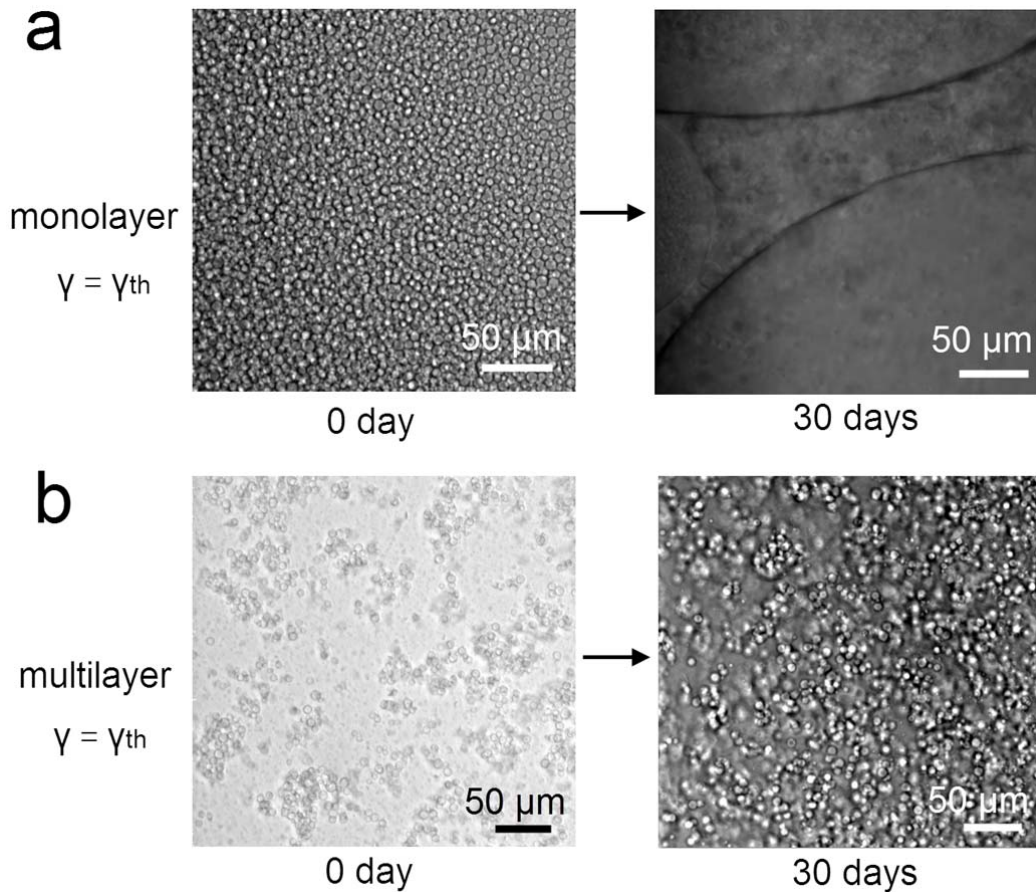
79 emulsion mixture at different concentrations and incubate the mixture at 65 °C.

80

81 **Supplementary Figure 6**

82 **Multilayered protein fibrils better stabilize w/w emulsions than monolayered fibrils**

83 **after 30 days of aging.**



84

85 **Supplementary Figure 6 | Optical microscope images of the w/w emulsions stabilized by**

86 **monolayered and multilayered fibrils. (a)** While a monolayer of fibril fails to stabilize w/w

87 emulsion after 30 days, **(b)** the multilayered fibrils can stabilize the w/w droplets and maintain

88 the initial droplet sizes. The interfacial tension of the w/w emulsion is kept at the threshold

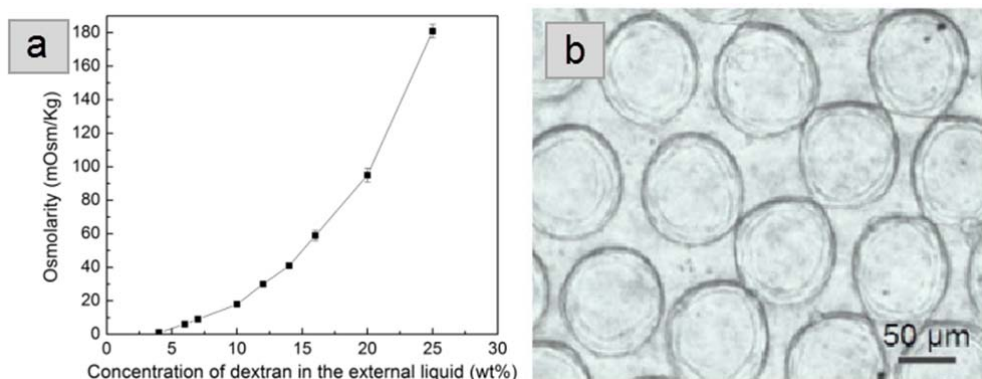
89 values for interfacial adsorption of single fibril,  $\gamma = \gamma_{th}$ . The compositions of the emulsion droplets

90 are denoted by point B in the phase diagram of figure 4f in the main text.

91

92

93 **Supplementary Figure 7**



94

95 **Supplementary Figure 7 | Osmotic shrinkage of the fibrillosomes** (a) Osmolarity of the dextran  
96 solution as a function of the concentration of dextran. (b) An optical microscope images showing  
97 the buckling morphology of the shrinking fibrillosomes in a hypertonic dextran solution (25 wt%,  
98 181 mOsm/Kg).

99

100 A 15 wt% dextran (48mOsm/Kg) solution is first encapsulated inside the fibrillosomes by using  
101 dextran-in-PEG emulsions as templates. To generate an osmotic pressure across the membrane  
102 of fibrillosomes, we transferred the fibrillosomes into different dextran solutions with their  
103 concentrations ranging from 4 wt% to 25 wt% (Reaching the solubility limit of dextran in water).  
104 The corresponding osmolarity of the dextran external liquid changes from near zero to  
105 181mOsm/Kg, as shown in the supplementary figure 7a. Due to the gradient in the concentration  
106 of dextran across the wall of the fibrillosomes, an osmotic pressure appears at the very beginning.  
107 The initial osmotic pressure can be calculated by using the osmolarity of the internal dextran  
108 solution minus that of the external dextran solution. With a positive osmotic pressure, water is  
109 sucked out of the fibrillosomes, leading to the shrinkage of fibrillosomes. On the contrary, the

110 fibrillosomes swell in a hypotonic dextran solution. Although dextran can slowly penetrate  
111 through the membrane of fibrillosomes, water diffuses across the membrane at a much faster  
112 speed, due to their much smaller sizes. Therefore, the osmotic effect still controls the swelling or  
113 shrinkage of fibrillosomes.

114

## 115 **Supplementary Note 1**

### 116 **A calculation on the adsorption energy of lysozyme monomers to the w/w interface**

117 We treat lysozyme monomers as sphere-shaped colloidal particles with the hydrodynamic  
118 diameter of 5 nm<sup>38</sup>. Ignoring the curvature of the W/W interface, the created area of W/W  
119 interface can be expressed as  $S_{w/w} = \pi r^2 \sin^2 \theta$ , and the removed dextran/fibril contact area  
120  $S_{dex} = 2\pi r^2 (1 - \cos \theta)$ . The adsorption energy of lysozyme monomer at W/W interface  
121 (desorption energy) can be calculated as<sup>11</sup>

#### 122 **Supplementary Equation 1:**

$$123 \quad \Delta G_{mono} = \pi r^2 \gamma_{w/w} (1 - |\cos \theta|)^2 \leq \pi r^2 \gamma_{w/w} = 3.14 \times \left(\frac{5nm}{2}\right)^2 \times 10^{-5} N / m = 2 \times 10^{-23} J$$

124 Where  $r$  is the hydrodynamic radius of lysozyme monomer, and  $\theta$  is the contact angle. The  
125 maximum desorption energy is acquired when  $\theta = 90^\circ$ .

126 However, this adsorption energy is still much less than the kinetic energy driving the  
127 detachment of lysozyme monomer from the w/w interface, which is estimated as

#### 128 **Supplementary Equation 2:**

$$129 \quad \Delta E_k = kT = 1.38 \times 10^{-23} J \cdot K^{-1} \times 300K = 4 \times 10^{-21} J$$

130 This suggests the thermal kinetic energy dominates the motion of monomers, and the  
131 monomers can freely enter and leave the interface with negligible energy compensation. The  
132 situation is equally established for monomers at all contact angles ( $0^\circ < \theta < 180^\circ$ ). According to



133 our theory, stabilizer of this kind can not form an effective barrier to prevent the direct contact of  
134 droplets or stabilize W/W emulsions.

135

136

137

138

139

140

## 141 **Supplementary Note 2**

142 **A calculation of the minimum thickness of fibril coating suggesting the stabilized W/W**

143 **emulsion droplets are coated by a monolayer of fibrils.** When the concentrations of fibrils are

144 kept at 0.025 wt%, 0.05 wt% and 0.075 wt%, the stabilized interfacial areas are approximately

145  $0.02 \text{ m}^2$ ,  $0.04 \text{ m}^2$  and  $0.06 \text{ m}^2$ , respectively (Fig. 2e in the main text). From the slope of the curve,

146 1 gram fibrils can stabilize an interfacial area of  $0.02 \text{ m}^2/0.025\% = 80 \text{ m}^2$ . Assuming the uniform

147 distribution of fibrils at W/W interface, the weight of fibrils covering an interfacial area of  $1 \text{ m}^2$  is

148  $1/80 = 0.0125 \text{ g}$ .

149 We suppose that the W/W emulsions are stabilized by fibril layers with a coverage ratio of  $C_f$ ,

150 then the weight of fibril layers coated on  $1 \text{ m}^2$  of the W/W interface,  $W_{fib}$ , can also be expressed

151 as,

152 **Supplementary Equation 3:**  $W_{fib} = \rho_{fib} V = \rho_{fib} (1 \text{ m}^2 \times C_{fib} \times d) = 0.0125 \text{ g}$ ,

153 where  $\rho_{fib}$  and  $V$  are the density and volume of the fibril layers;  $d$  is the height of fibril layers

154 packed at the W/W interface. Density of fibril layers,  $\rho_{fib}$ , is estimated as  $1.03 \pm 0.02 \text{ g/cm}^3$ . When

155 a mixture solution of dextran, PEG, and fibrils is centrifuged at a high rotation rate (6500 rpm), a

156 fibril-rich phase is formed between the PEG-rich top phase and the dextran-rich bottom phase,  
 157 suggesting the density of fibril-rich phase is between the dextran-rich ( $\rho_{dex} = 1.057 \text{ g/cm}^3$ ) and the  
 158 PEG-rich phase ( $\rho_{PEG} = 1.01 \text{ g/cm}^3$ ). The coverage ratio of fibrils,  $C_{fib}$ , is approximately 60-70 %,  
 159 which can be measured roughly from SEM images (Fig. 2f). Therefore, thickness of the fibril layers  
 160 at the W/W interface,  $T_{fib}$  can be predicted as:

161 **Supplementary Equation 4:**  $T_{fib} = W_{fib} / [\rho_{fib} (1 \text{ m}^2 \times C_{fib})] = 0.0125 / (1.03 \times 10^6 \times 0.7) = 1.7 \times 10^{-8} \text{ m}$

162 The resultant thickness of fibril layer (17 nm) is approximately equal to the fibril width (15  
 163 nm), suggesting that stabilization of W/W emulsions require a monolayer of fibrils to cover the  
 164 interface. This prediction is also confirmed from the SEM observation (Fig. 2d).

165

### 166 **Supplementary Note 3**

#### 167 **A model for calculating the adsorption energy of single fibril at the W/W interface**

168

169

170

171

172 When a single piece of fibril leaves the W/W interface and enters the PEG-rich continuous  
 173 phase, the adsorption/desorption energy can be estimated from the change in the total  
 174 interfacial energy, as illustrated in the Supplementary Figure 3a. By accounting for the eliminated  
 175 area of W/W interface ( $S_{W/W}$ ) and the created PEG/fibril contact area ( $S_{PEG/fib}$ ), the free energy  
 176 change can be expressed as

177 **Supplementary Equation 5:**  $\Delta G_{fibril} = \gamma_{w/w} S_{w/w} + S_{dex} (\gamma_{PEG/fib} - \gamma_{dex/fib})$

178 Ignoring the curvature of the W/W interface for simplicity, these areas are expressed as  $S_{W/W}$   
179  $= 2RL\sin\alpha$  and  $S_{dex} = 2\alpha RL$ , where  $2R$  (15 nm) is the cross-sectional diameter of fibrils,  $L$  (600 nm,  
180 Supplementary Figure 1) is the average length of fibrils and  $2\alpha$  is the angle subtended by the two  
181 three-phase contact lines. The fibril contact angle,  $\theta$ , is the supplementary angle of  $\alpha$  in the  
182 Supplementary Figure 3a,  $\theta + \alpha = \pi$ . Since the contact angle cannot be easily measured directly,  
183 due to the small sizes of fibrils, we deposited a film of lysozyme fibrils on a solid substrate and  
184 measured the wetting angle of a dextran-rich droplet at the PEG/fibrils interface. The measured  
185 wetting angle is  $142^\circ \pm 7^\circ$  (see supplementary Figure 3b). This contact angle remains almost  
186 constant as the equilibrium concentrations of the two aqueous phases change. A static force  
187 equilibrium along the radial direction of the fibrils results in the following relationship,

188 **Supplementary Equation 6:**  $\gamma_{PEG/fib} - \gamma_{dex/fib} + \gamma_{w/w} \cos(\pi - \theta) = 0$ .

189 Combining Supplementary Equations 5 and 6, the adsorption energy can be expressed as,

190 **Supplementary Equation 7:**  $\Delta G_{fibril} = 2R\gamma_{w/w}L(\sin\theta + \pi\cos\theta - \theta\cos\theta)$ .

191

192

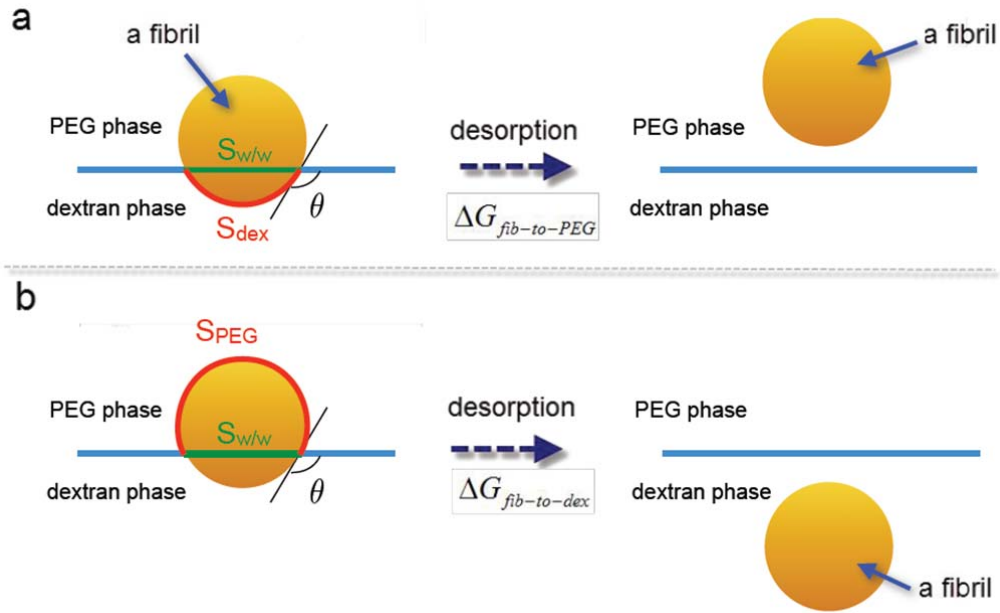
193

194

195

#### 196 **Supplementary Note 4**

197 **A physical model to calculate the energy barriers for coalescence of dextran-in-PEG emulsion**  
198 **and PEG-in-dextran emulsion.**



199

200 **Supplementary Schematic 1: Desorption of fibrils from W/W interface when two adjacent**

201 **droplet coalesce. (a)** Coalescence of two PEG-in-dextran drops requires fibrils to detach from

202 W/W interface and enter the PEG-rich droplet phase. The corresponding desorption energy is

203 expressed as  $\Delta G_{fib-to-PEG}$ ; **(b)** Coalescence of two dextran-in-PEG drops requires fibrils to detach

204 from W/W interface and enter into the dextran-rich droplet phase. The desorption energy in this

205 process is expressed as  $\Delta G_{fib-to-dex}$ .

206 Interfaces of two adjacent emulsion droplets must touch before they can merge into a single

207 droplet. The role of fibrils is to form a physical barrier that separates the two interfaces. When

208 two dextran-in-PEG emulsion drops approach with each other, the fibrils transiently desorb from

209 W/W interface and enter either the PEG-rich continuous phase or the dextran-rich droplet phase.

210 If fibrils transiently enter the PEG-rich continuous phase, they will separate the two dextran-rich

211 droplets and prevent their direct contact. To coalesce, fibrils must enter the dextran-rich phase;

212 however, this often requires consuming higher energy than entering to the PEG-rich phase,

213 deduced from the calculation on the interfacial energy in the following paragraph.

214 When a single fibril transiently leave the W/W interface and enter the PEG-rich phase, the  
 215 desorption energy can be estimated from the change in the total interfacial energy, as illustrated  
 216 in Supplementary Schematic 1a. By accounting for the eliminated area of W/W interface ( $S_{W/W}$ )  
 217 and the created PEG/fibril contact area ( $S_{PEG/fib}$ ), the free energy change can be expressed as

218 **Supplementary Equation 8:**  $\Delta G_{fib-to-PEG} = \gamma_{w/w} S_{w/w} + S_{dex} (\gamma_{peg/fib} - \gamma_{dex/fib})$

219 Assuming a flat interface, the contact area of a fibril to the dextran-rich phase is calculated as

220 **Supplementary Equation 9:**  $S_{dex} = 2\alpha RL$ .

221 Such that Supplementary Equation 8 becomes

222 **Supplementary Equation 10:**  $\Delta G_{fib-to-PEG} = 2R\gamma_{w/w} L(\sin\theta + \pi \cos\theta - \theta \cos\theta) = 0.186\gamma_{w/w} RL$

223 Instead, when a single fibril transiently enters the dextran-rich emulsion phase, the associated  
 224 desorption energy (see Supplementary Schematic 1b) can be estimated by

225 **Supplementary Equation 11:**  $\Delta G_{fib-to-dex} = \gamma_{w/w} S_{w/w} + S_{peg} (\gamma_{dex/fib} - \gamma_{peg/fib})$

226 Assuming a flat interface, the contact area of a fibril to the PEG-rich phase is calculated as,

227 **Supplementary Equation 12:**  $S_{PEG} = 2(\pi - \alpha)RL$ .

228 Such that Supplementary Equation 11 becomes

229 **Supplementary Equation 13:**  $\Delta G_{fib-to-dex} = \gamma_{w/w} DL[\sin\alpha + (\pi - \alpha) \cdot \cos(\pi - \theta)] = 5.14\gamma_{w/w} RL$

230

231 By comparing the desorption energy under the two conditions, the energetic cost is 25 times  
 232 for getting a single fibril into the dextran-rich phase than to the PEG-rich phase. This explains why  
 233 fibrils preferentially partition in the PEG-rich phase upon destabilization.

234 The calculation also denotes that the dextran-in-PEG emulsions must overcome a high energy  
 235 barrier before coalescence can occur. In comparison, coalescence of PEG-in-dextran emulsions

236 occurs more easily because of the low energy barrier for fibrils to transiently enter the PEG-rich  
237 emulsion phase. Therefore, even with the same interfacial tension and calculated adsorption  
238 energy, fibril-coated dextran-in-PEG emulsion droplets are much more stable than the  
239 PEG-in-dextran emulsion droplets. However, when the interfacial tension declines to near zero,  
240 both of the two kinds of energy barrier becomes negligible compared to thermal energy. In this  
241 condition, fibrils almost distribute homogenously in the mixture.  
242